JOC The Journal of Organic Chemistry

Article

pubs.acs.org/joc

Cone Calix[4]arenes with Orientable Glycosylthioureido Groups at the Upper Rim: An In-Depth Analysis of Their Symmetry Properties

Laura Legnani,[†] Federica Compostella,[‡] Francesco Sansone,[§] and Lucio Toma*[,†]

[†]Dipartimento di Chimica, Università di Pavia, Via Taramelli 12, 27100 Pavia, Italy

[‡]Dipartimento di Biotecnologie Mediche e Medicina Traslazionale, Università di Milano, Via Saldini 50, 20133 Milano, Italy

[§]Dipartimento di Chimica, Università di Parma, Parco Area delle Scienze 17/A, 43124 Parma, Italy

Supporting Information

ABSTRACT: The two glycoclusters α- and β-D-mannosylthioureidocalix[4]arenes **1** and **2** in the *cone* geometry have been submitted to a conformational investigation with the DFT approach at the standard B3LYP/6-31G(d) level and using a water continuum solvent model. After a reasoned choice of the level of calculation and the evaluation of the properties of the monomeric components of **1** and **2**, the intrinsic conformational properties of *cone* calix[4]arenes with orientable groups at the upper rim were thoroughly analyzed. From the possible combinations of the directions that the groups may assume, 10 different geometries derive, all chiral. These geometries are interchangeable through two different processes, named breathing equilibrium and arrow rotation, that allow a dense network connection among them. When the modeling of whole macrocycles **1** and **2** was performed, a huge difference in their conformational behavior that heavily influences the presentation mode of their saccharidic moieties was found.

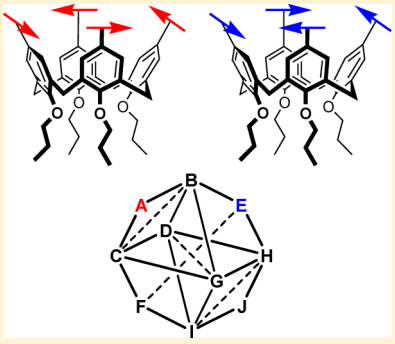

INTRODUCTION

Multivalent presentation of carbohydrates using suitable conjugation chemistry and scaffold selection may result in a better efficiency and a higher selectivity in the interaction with the corresponding receptors such as lectins and immunoglobulins. The substituents linked to the scaffolds work as fingers that may diverge from the central core or orient themselves parallel to each other and converge toward one or more units of a partner to interact with it. The nature of the scaffolds plays a crucial role in the presentation of the substituents as well as the nature of the linkers that connect to them. Calix[*n*]arenes, for example, a well-known class of macrocycles, besides a series of other applications,[1] have been successfully used as scaffolds for multivalent presentation of saccharide moieties.[2,3] The even-numbered macrocycles (n = 4, 6, and 8) have been mostly used. The smallest member of this family of macrocycles (n = 4) has the lowest mobility and, if the alkoxy groups at the lower rim are large enough, stable conformational isomers that allow a controlled display of the saccharide units in the space exist. Several linkers with different flexibility have been exploited to connect sugars to calixarenes.[2,3] The more rigid ones can heavily constrain the orientation options of the substituents so that their presentation mode may be strongly affected.

In the literature, several glycocalix[*n*]arenes in which glycosyl moieties such as glucose, galactose, or lactose are linked as β anomers, through a thiourea unit, to the upper rim of these macrocyclic platforms have been reported.[4−10] Despite of, or perhaps because of, the proximity of the sugar epitopes to the calixarene cavity, these glycosylthioureidocalixarenes have shown in some cases very interesting inhibition properties toward specific carbohydrate recognition proteins. Together with a high efficiency often associated with a significant multivalent effect, an impressive selectivity has been also observed,[4] for instance in the binding of medically relevant lectins, namely galectins, belonging to the same family. It is interesting that the resulting selectivity strongly related to the size and geometry of the glycocalixarene. Tetralactosylcalix[4]-arenes blocked in the *cone* geometry, i.e., that orienting the aryl groups in the same direction, showed[4,5] for example a strong inhibition activity against galectin-3 and no activity against galectin-1.

Another interesting point observed in the previous studies is that a synthetic spacer like thiourea seems, at least in part, to modify the natural specificity of the receptor for the substrate. β-Glucosylthioureidocalixarenes were in fact able to interact with concanavalin A, a lectin known to be selective for natural α-manno- and α-glucosides.[6,8]

On the basis of these data showing that glycosylthiour-eidocalixarenes indeed make up an interesting class of selective multivalent ligands, we focused on the *cone* calix[4]arene scaffold and decided to investigate from a conformational point of view the two glycoclusters **1** and **2**, both exposing mannosyl moieties but differing in their anomeric configurations. Because of the relevance of mannose in biology, these clusters could be in the future synthesized and studied as inhibitors of lectins involved in important processes. Actually, cluster **1**, where mannose is present in the α-anomeric configuration, has

Received: April 20, 2015
Published: July 8, 2015

DOI: 10.1021/acs.joc.5b00878
J. Org. Chem. 2015, 80, 7412−7418

Chart 1

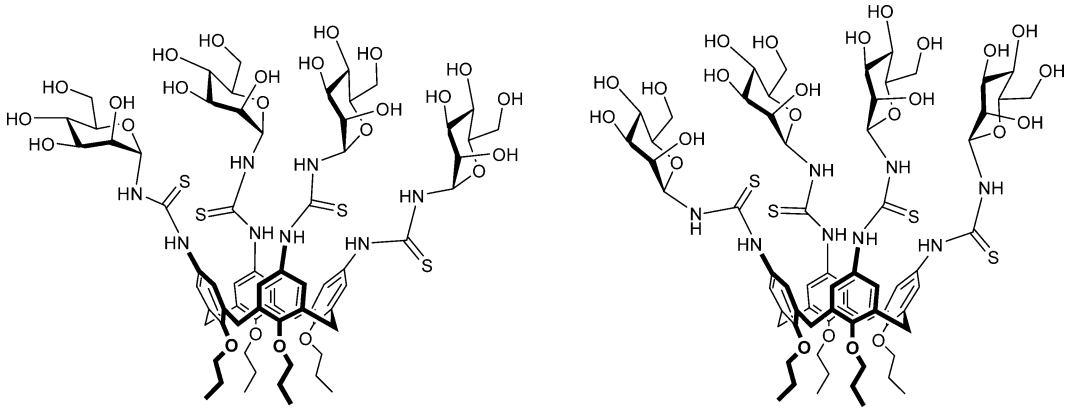

recently been reported for the preparation of multivalent gold nanoparticles.[11] On the other hand, to the best of our knowledge, thioureidocalix[4]arene **2** containing β-mannosyl moieties has never been synthesized. In a sort of predictive challenge, in this investigation the two potential multivalent ligands have been compared to gain insight into the effects of the anomeric configuration of the sugar on the presentation mode of the saccharide portion of glycoclusters.

Thus, we have undertaken an in-depth theoretical study of α- and β-D-mannosylthioureidocalix[4]arenes **1** and **2** (Chart 1) and, following our usual approach to dissecting the problem in all its components, we have faced step by step the several computational items involved in the study: the choice of the suitable level of calculation, the evaluation of the properties of each monomeric component of calixarenes **1** and **2**, the need to deepen the knowledge of the intrinsic conformational properties of *cone* calix[4]arenes with orientable groups at the upper rim, and, just at the end, modeling whole macrocycles **1** and **2**, including their chiral mannosyl moieties.

RESULTS AND DISCUSSION

Choice of the Computational Method. In a modeling study, the choice of the computational approach is of utmost importance for a correct description of the system. In the framework of the widely used density functional theory, attention was focused on the standard B3LYP/6-31G(d) level[12,13] as the large molecular size of **1** and **2** did not allow the use of higher theory levels, which would cause unreasonably longer computational time. The first goal was to verify the suitability of this approach in correctly describing the different functionalities in the molecules, i.e., the thioureido groups and the glycosides. In the thioureido units, the restricted rotation of the pseudoamide NH-C=S bonds and the consequent tendency to planarity allow the existence of the four geometrical isomers designated as *ZZ*, *ZE*, *EZ*, and *EE*. An extensive MP2/aug-cc-pVDZ study[14] of alkyl- and phenyl-substituted thiourea derivatives showed that conformations with alkyl groups *Z* to the sulfur atom are more stable by 0.4–1.5 kcal/mol than the *E* forms. In contrast, analysis of phenylthiourea revealed that in this case the opposite *E* isomer is preferred by 2.65 kcal/mol.

In compounds **1** and **2**, the substituents at the two sides of thiourea are a *p*-propoxyphenyl and a glycan. In analogy with the MP2 data for phenylthiourea mentioned above, a propoxyphenylthiourea should present a clear preference for the *E* geometry. To the best of our knowledge, no calculations at the MP2 level of theory have been performed on glycosylthioureas, so that their conformational preferences have to be investigated. Therefore, we decided to model at this level the simplified structures **3** and **4** (Chart 2). They present a

Chart 2

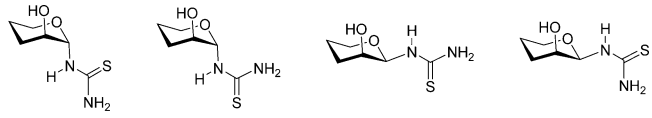

thiourea at the anomeric position in the α or β orientation, respectively, and an axially oriented hydroxyl group at position 2 of a pyranose ring in the $^4C_1$ conformation, maintaining the main structural features required for a correct description of the mannosyl–thiourea interaction.

The *E* and *Z* geometries of compounds **3** and **4** were built and optimized at the MP2/aug-cc-pVDZ level. Table 1 reports

Table 1. Relative Energies (kilocalories per mole) of the *E* and *Z* Geometries of Compounds 3 and 4 Optimized at Different Levels of Theory

	MP2/aug-cc-pVDZ	B3LYP/6-31G(d)	B3LYP/6-31G(d)[a]
E-**3**	0.00	0.00	0.00
Z-**3**	6.35	7.23	3.42
E-**4**	0.00	0.00	0.00
Z-**4**	1.53	2.30	1.57
E-phenylthiourea	0.00[b]	0.00	0.00
Z-phenylthiourea	2.65[b]	3.92	2.54

[a]Optimization performed in a polarizable continuum solvent model (PCM) choosing water as the solvent. [b]Data from ref 14.

the relative energies of the optimized structures. In both cases, the *E* geometry is preferred over the *Z* one. Then we tested the DFT B3LYP functional, using the 6-31G(d) basis set, for its ability to reproduce the MP2 stability data; thus, we optimized in vacuum, at this level of theory, each couple of *E*/*Z* isomers of thioureas **3** and **4** as well as phenylthiourea (Table 1). The DFT approach was able to reproduce the greater stability of the *E* isomer of the three computed N-substituted thioureas with an energy difference even greater than that computed at the

DOI: 10.1021/acs.joc.5b00878
J. Org. Chem. 2015, 80, 7412–7418

Chart 3

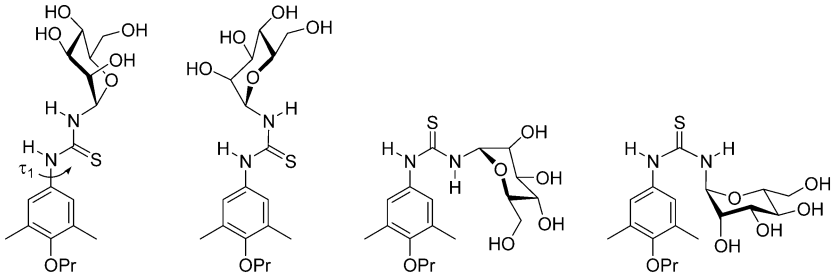

MP2 level. Moreover, considering that vacuum optimization on saccharide compounds might be biased by the excessive strength of the hydrogen bonds involving the hydroxyl groups, the structures were optimized again taking into consideration the solvent effect by using a polarizable continuum model (PCM)[15−17] and choosing water as the solvent. Once more, the *E* isomers were more stable, though the values of the relative energy of the *Z* isomers were smaller than in the in vacuum optimizations. It is worth pointing out that the DFT approach combined with the solvent effect gives results comparable with those obtained with the MP2 approach over a much shorter computational time. Thus, throughout this work, all calculations were performed at the B3LYP/6-31G(d) level through optimizations in the PCM solvent model of water.

Modeling of Monomers 5 and 6. In a stepwise approach to the study of the entire calixarenes, the conformational behavior of the single model monomeric α- and β-D-mannosylthioureas **5** and **6** (Chart 3) was investigated and the results are reported in Table 2. The aryl and glycosyl groups

Table 2. Relative Energies (kilocalories per mole) of the Four Geometrical Isomers of Compounds 5 and 6 Optimized at the B3LYP/6-31G(d) Level in a Water Continuum Solvent Model

	ZZ-a	*ZE-a*	*EZ-a*	*EE-a*	*ZZ-b*	*ZE-b*	*EZ-b*	*EE-b*
5	3.48	0.00	0.56	7.31	3.48	0.80	0.66	4.77
6	2.84	*a*	0.00	4.36	2.84	0.95	0.02	4.98

[a]Minimum not located. It converges to the *ZE-b* conformer during the optimization.

on the two sides of thiourea should have, as discussed above, a defined preference for the *E* geometry at the respective pseudoamide NH-C═S bond. Indeed, the *EE* geometry suffers from a severe steric strain involving the aryl and sugar moieties that is in part released through a deviation from planarity of the thioureido group, leading to stereoelectronic destabilization. Despite this balance between steric and stereoelectronic factors, the *EE* arrangement becomes the least stable one. Therefore, structures having one NH-C═S bond in the *E* geometry and the other in the *Z* geometry are found to be the global minima for both **5** and **6**, with the *ZE* geometry preferred by **5** and the *EZ* geometry by its β-anomer **6** (Table 2). This different behavior is a consequence of the relative stability of the *E* and *Z* isomers reported in Table 1, where it is shown that the $E - Z$ energy difference for **3** is larger than for phenylthiourea, while it is the opposite in the case for **4**, which shows a smaller $E - Z$ energy difference. The *ZZ* geometry was found to be less stable than the global minimum by ∼3 kcal/mol in both compounds.

The three-dimensional plots reported in Figure 1 show that the *ZZ* and *ZE* geometries determine an almost extended shape for the molecules that, on the contrary, assume a bent shape in the *EZ* and *EE* geometries; in the latter cases, the steric strain between the sugar and the phenyl ring is released by deviation of thiourea from planarity. Moreover, because of conjugation, there is the tendency of thiourea and phenyl to coplanarity; this tendency is hindered by the interactions of the phenyl *meta* hydrogens with the NH hydrogen or the CS sulfur atoms that lead to a plane between the two groups of approximately 50−60°. Thus, for each thiourea geometry, there are two possible orientations with respect to phenyl that are not isoenergetic because of the chirality of the monosaccharide. They are distinguished by the descriptors *a* and *b* in Table 2 and Figure 1, assigned on the basis of the dihedral angle τ_1, defined by the atoms C3−C4−N−C(═S) (Chart 3), with *a* used for $90° < \tau_1 < 270°$ and *b* for $-90° < \tau_1 < 90°$.

Symmetry Properties of *cone*-Calix[4]arenes Substituted at the Upper Rim. When four propoxy groups are present at the lower rim of calix[4]arenes, as in the case of **1** and **2**, the macrocycle is locked in specific conformations, named by Gutsche[18] as *cone*, partial *cone*, 1,3-alternate, and 1,2-alternate, differing for the orientation of the phenyl groups. In the *cone* conformation, the four aryl groups are oriented in the same direction, giving rise to a geometry usually represented as a C_4 symmetrical structure. However, the minimum energy geometry is better described as a C_2 symmetrical structure, the

DOI: 10.1021/acs.joc.5b00878
J. Org. Chem. 2015, 80, 7412−7418

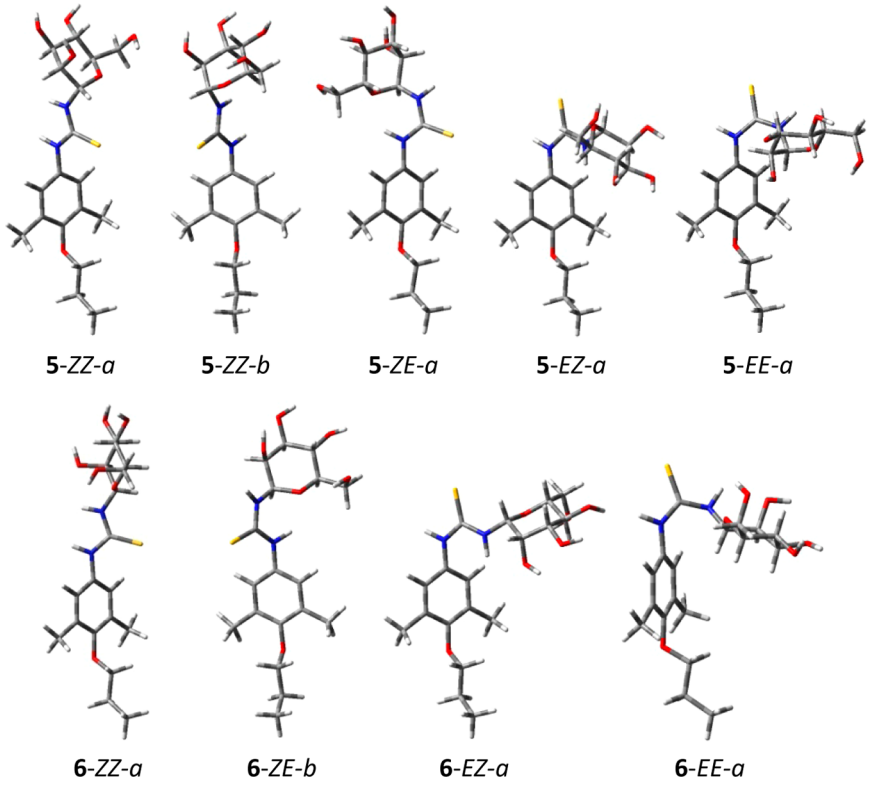

Figure 1. Three-dimensional plot of the *ZZ*, *ZE*, *EZ*, and *EE* conformers of monomeric α- and β-D-mannosylthioureas **5** and **6**.

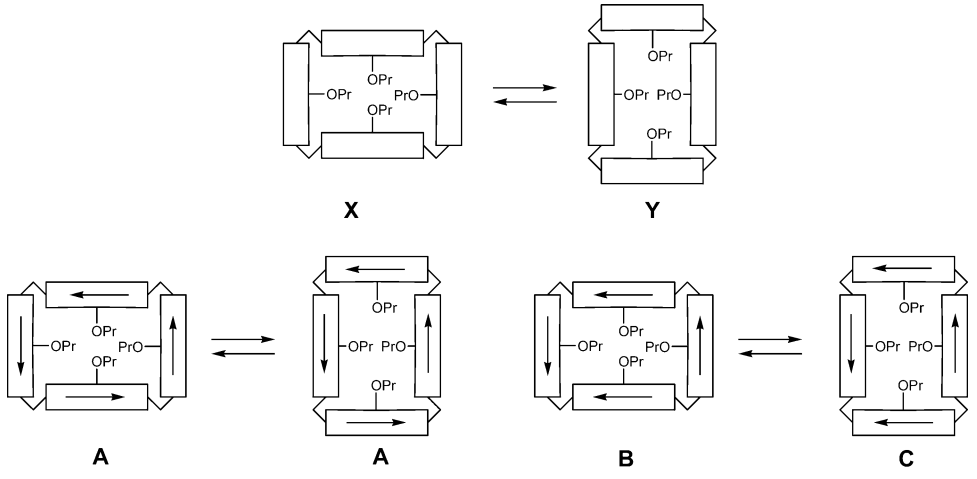

Figure 2. Schematic representation of the breathing equilibrium of *cone*-calix[4]arenes without (**X** and **Y**) and with (**A**–**C**) orientable groups at the upper rim.

so-called *pinched cone* conformation, that has two opposite phenyl groups at a distance much shorter than that between the other two. However, an easy equilibrium, in which the farther groups have approached and the closer ones have moved away, interchanges the close and far phenyl groups, making them indistinguishable.[19] This equilibrium between the *pinched cone* conformations, which could be called the breathing equilibrium, can be schematically represented using rectangular-shaped drawings in which the macrocycle is seen from a top view (Figure 2, **X** ⇆ **Y** equilibrium).

The **X** and **Y** structures are indistinguishable but, when at the upper rim of calixarene are introduced groups that may assume two different orientations with respect to the phenyl rings, as for example the thiourea groups, a series of distinguishable conformers can exist. In Figure 2, the orientable groups are represented as arrows that can be arranged in combinations such as those indicated as **A**–**C**. The breathing equilibrium on these structures may produce a conformer indistinguishable from the starting one, as in the case of **A**, or a distinct conformer, as in the **B** ⇆ **C** equilibrium. A total of 10 different combinations do exist; these 10 conformers, **A**–**J**, are drawn in a simpler, more schematic, way in Figure 3. The conformers can interconvert through the breathing equilibrium (**B**/**C**, **D**/**G**, **E**/**F**, and **H**/**I**) or through the rotation of an orientable group (arrow) with respect to the phenyl group to which it is linked. For example, **A** can be converted into **B** or **C** through the rotation of just one arrow; in turn, **B** can be converted into **D**, **E**, or **G**, etc. These transformations can be represented by a

DOI: 10.1021/acs.joc.5b00878
J. Org. Chem. 2015, 80, 7412–7418

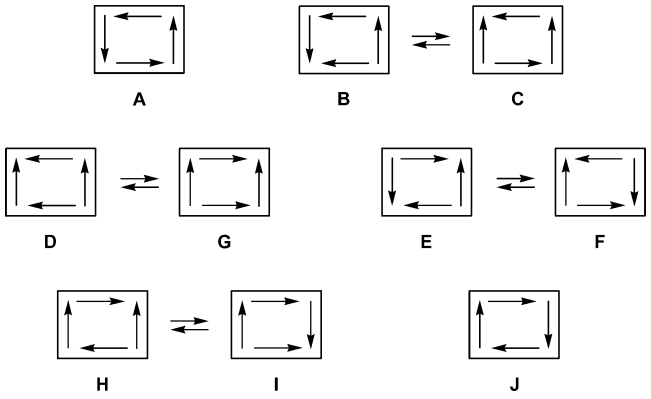

Figure 3. Schematic representation of the 10 conformations (**A**–**J**) of a *cone*-calix[4]arene with four orientable groups at the upper rim.

graph (Figure 4) in which each solid line connects conformers that can be interchanged through rotation of an arrow and the

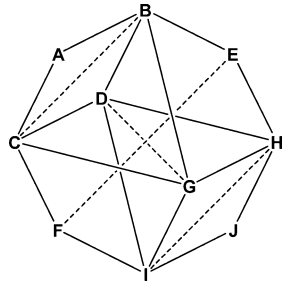

Figure 4. Graph representing the connections among the 10 **A**–**J** conformations of a *cone*-calix[4]arene with four orientable groups at the upper rim through arrow rotations (solid lines) or breathing equilibria (dashed lines).

dashed lines connect conformers that can be interchanged through the breathing equilibrium. At the two extremes are the counterclockwise (**A**) and clockwise (**J**) arrow arrangements that obviously require four arrow rotations to be converted one into the other.

All of the **A**–**J** geometries are chiral. Moreover, they can be grouped into five enantiomeric pairs, **A** and **J**, **B** and **I**, **C** and **H**, **D** and **G**, and **E** and **F**; i.e., all the pairs at the opposite vertices of the graph of Figure 4 are enantiomerically related and hence isoenergetic. When the orientable groups contain chiral elements, all of the **A**–**J** geometries become diastereoisomeric so that each of them presents a different energy value.

Modeling of Calixarenes 1 and 2. The complete structures of α- and β-D-mannosylthioureidocalix[4]arenes (**1** and **2**) were then built on the basis of the optimized monomeric structures **5** and **6** and taking into account the symmetry properties of *cone* calixarenes with orientable groups at the upper rim discussed above. The complete exploration of the conformational space of **1** and **2** through a systematic search approach may become very demanding. However, we decided to use this approach, instead of a molecular dynamics approach based on an empirical force field method, to guarantee an appropriate description of the different functionalities present in the molecules, in particular the thiourea groups. The procedure first exemplified for **1** was successively applied to compound **2**.

Thus, we built starting geometries for α-D-mannosylthioureidocalix[4]arene **1** based on the energy minimum conformers of compound **5**, by selecting the *ZE* geometry for the thiourea and considering that the *ZE-a* and *ZE-b* geometries correspond to the right- and left-oriented arrows, respectively, in the schematic representations in Figure 3 when observed from a point of view external to the calix core. First, a geometry of **A** type was built, i.e., *ZE-a* geometries for the orientation of the four thiourea groups. It was optimized at the same calculation level used for the monomers, yielding the **1A**-*ZE* conformer reported in Figure 5.

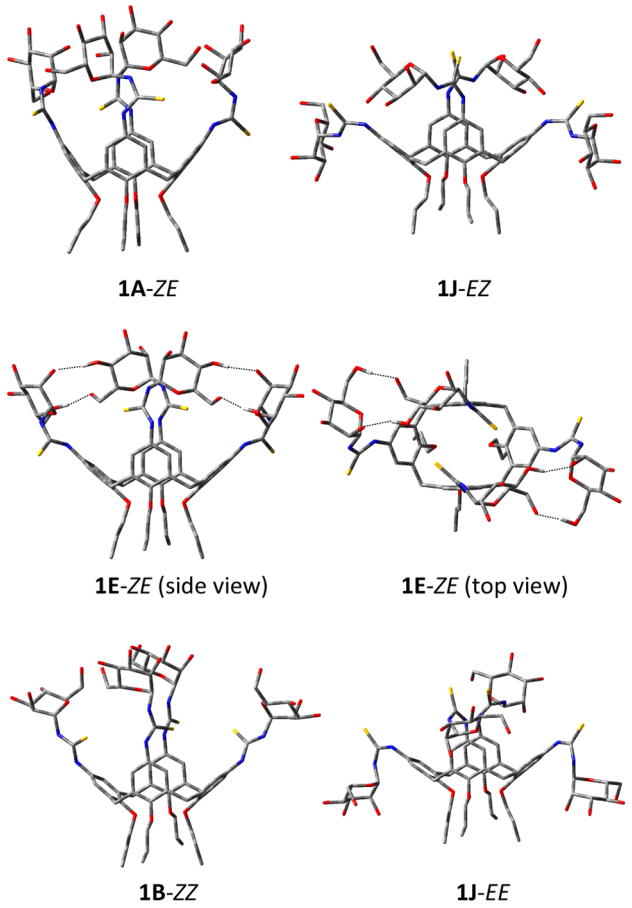

Figure 5. Three-dimensional plots of conformers **1A**-*ZE*, **1E**-*ZE*, **1J**-*EZ*, **1B**-*ZZ*, and **1J**-*EE* of α-D-mannosylthioureidocalix[4]arene **1**. The hydrogen atoms have been omitted for the sake of clarity except those involved in the inter-residue H-bonds of **1E**-*ZE*.

From this conformer, nine new starting geometries were built up, through suitable rotations of the thiourea groups with respect to the corresponding phenyl group (arrow rotations), and optimized. The relative energies of all 10 minimum energy conformers so obtained are reported in Table 1S (Supporting Information) together with the percentage populations at 298 K calculated with the Boltzmann equation. The global minimum, conformer **1E**-*ZE*, was largely preferred. In fact, the second and third conformers, **1C**-*ZE* and **1A**-*ZE*, respectively, were less stable by 3.09 and 4.43 kcal/mol, respectively, so that **1E**-*ZE* accounts for more than 99% of the overall population. Its three-dimensional plot is reported in Figure 5, whereas those of the other conformers are reported in Figure 1S (Supporting Information). Conformer **1E**-*ZE* has a C_2 symmetrical geometry with adjacent couples of mannosyl residues interacting through hydrogen bonds. It is noteworthy

DOI: 10.1021/acs.joc.5b00878
J. Org. Chem. 2015, 80, 7412–7418

that the four mannosyl residues are not equivalent, each couple being identical at the opposite sides of the molecule; in fact, two residues expose their β-face outward and the other two their α-face. As shown in the graph in Figure 4, to interchange these two residues, at least one breathing equilibrium and four arrow rotations are necessary, passing through four conformers with energies higher than that of **1E**-*ZE* (Scheme 1S, Supporting Information). Therefore, the interchange of the two couples of residues should be rather difficult as a series of arrow rotations are necessary; moreover, these are much more difficult in **1E**-*ZE* than in monomer **5** as they require the breaking of the network of inter-residue hydrogen bonds.

Though the *ZE* orientation of the thiourea is preferred in monomer **5**, it is necessary to ascertain that this conformational preference is maintained in **1**. Thus, the procedure described above for the *ZE* geometry was repeated for the three other thiourea geometries optimizing in each case the 10 corresponding **A**−**J** conformations; the data of the preferred conformer for each thiourea geometry, **1J**-*EZ*, **1B**-*ZZ*, and **1J**-*EE*, are reported in Table 1S (Supporting Information). All these geometries were shown to be much less stable than **1E**-*ZE*, their relative energies being 9.19, 12.06, and 33.00 kcal/mol, respectively. Their three-dimensional plots are reported in Figure 5.

The approach used for the modeling of compound **1** was then applied to β-D-mannosylthioureidocalix[4]arene **2**, and the results are summarized in Table 2S and Figure 2S (Supporting Information). In this case, a definite preference for the *EZ* geometry of the thiourea group was found and the global minimum conformer, accounting for almost 90% of the overall population, was shown to be **2A**-*EZ* (Figure 6), with the

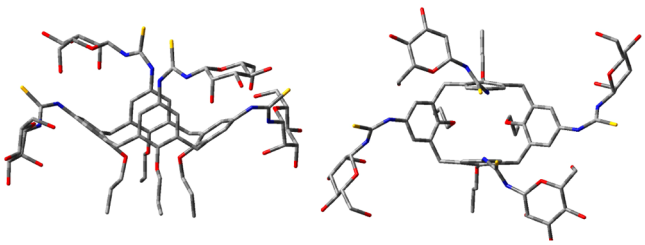

Figure 6. Three-dimensional plots of the global minimum conformer **2A**-*EZ* of β-D-mannosylthioureidocalix[4]arene **2**. The hydrogen atoms have been omitted for the sake of clarity.

remaining 10% attributable to its **2G**-*EZ*, **2B**-*EZ*, and **2E**-*EZ* graph neighbors. The other thiourea geometries were shown to be less stable; in fact, the corresponding preferred **2I**-*ZE*, **2I**-*ZZ*, and **2A**-*EE* conformers showed relative energy values of 5.67, 8.84, and 25.56 kcal/mol, respectively. As for calixarene **1**, the global minimum conformer of calixarene **2**, **2A**-*EZ*, has a C_2 symmetrical geometry with two couples of identical opposite β-mannosyl residues. However, it should be noted that in conformer **2A**-*EZ* these residues point outward with respect to the calix core so that no inter-residue hydrogen bond can be established. This allows a certain degree of conformational mobility that makes the arrow rotations easier than in the case of the α-anomer.[20] Moreover, the two couples of sugar residues can easily interconvert; in fact, the breathing equilibrium from **2A**-*EZ* yields an identical **A**-type geometry with interchanged mannose residues (Scheme 2S, Supporting Information), thus making the four sugar residues actually indistinguishable.[21]

CONCLUSIONS

With the final goal of investigating the conformational properties of two α- and β-mannosyl glycoclusters, and highlighting their similarities and differences, we had to deal with the problem of the multiple arrangements allowed to *cone* calix[4]arenes functionalized with orientable groups at the upper rim. A systematic analysis of the possible orientations of these groups evidenced specific symmetry properties that can heavily influence the overall conformational behavior.

A restricted rotation around the bond connecting the phenyl groups of calixarenes to the functionality at their 4 position allows the definition of the substituent as an orientable group when this functionality is nonsymmetric in its nature. The presence of orientable groups at the upper rim gives rise to 10 different geometries schematically represented as **A**−**J** in Figure 3. These geometries are chiral structures corresponding to five enantiomeric pairs. Their interconversion relies onto two different processes, the breathing equilibrium and the arrow rotation. Depending on the extent of conjugation of the orientable group with the phenyl and the possibility of the groups linked to the calixarene structure to establish through-space interaction such as hydrogen bonds, the 10 geometries (**A**−**J**) are more or less easily interconvertible.

The theoretical study of α- and β-D-mannosylthioureidocalix[4]arenes **1** and **2** evidenced a huge difference in their conformational behavior that heavily influences the presentation mode of the saccharidic moieties. The preference of **1** for the *ZE* geometry of thiourea determines an extended shape of each monomeric unit. This allows the formation of hydrogen bonds between adjacent couples of mannosyl residues. The optimal orientation of these residues corresponds to that defined by the **E**-type geometry in which hydrogen bonds are established among the hydroxyl groups at positions 4 and 6 of one residue and those at positions 6 and 2 of the other. Moreover, the residues expose alternatively their α or β face outward, and consequently, the four mannosyl residues are not equivalent. The β-isomer **2**, conversely, shows a neat preference for the *EZ* geometry of thiourea with a bent shape that turns the mannosyl residues away from the calixarene core preventing the formation of any inter-residue hydrogen bond. Consequently, **2** prefers the **A**-type geometry in which the four mannosyl residues can easily be interchanged simply through a breathing equilibrium between two *pinched cone* conformers.

In conclusion, though the two isomeric glycoclusters differ only in the anomeric configuration of the sugar, a great difference in their overall geometry has been evidenced so that a very different ability to interact with a protein partner can be hypothesized, in a manner independent of the native selectivity of the receptor observed for one anomer or the other in natural substrates. This shows that the preliminary knowledge of the conformational properties of a calixarene glycocluster can become a powerful tool in driving the synthetic work toward the targets that are predicted to better fit the desired features for a useful multivalent presentation.

COMPUTATIONAL METHODS

All the calculations were conducted using the Gaussian09 program package.[22] All the structures were optimized at the B3LYP/6-31G(d) level[12,13] in the water solvent simulated using a self-consistent reaction field (SCRF) method, based on a polarizable continuum solvent model (PCM).[15−17]

DOI: 10.1021/acs.joc.5b00878
J. Org. Chem. 2015, 80, 7412−7418

■ ASSOCIATED CONTENT

Supporting Information

Schemes 1S and 2S, Tables 1S and 2S, Figures 1S and 2S, and electronic energy and Cartesian coordinates of all computed structures. The Supporting Information is available free of charge on the ACS Publications website at DOI: 10.1021/acs.joc.5b00878.

■ AUTHOR INFORMATION

Corresponding Author

*E-mail: lucio.toma@unipv.it. Telephone: (+39) 0382987843. Fax: (+39) 0382987323.

Notes

The authors declare no competing financial interest.

■ ACKNOWLEDGMENTS

The Italian Ministry of University and Research (Grant PRIN 2010-11, prot. 2010JMAZML, Italian network for the development of multivalent nanosystems) is gratefully acknowledged for financial support. CINECA is also acknowledged for the allocation of computer time.

■ REFERENCES

(1) Sansone, F.; Baldini, L.; Casnati, A.; Ungaro, R. *New J. Chem.* **2010**, *34*, 2715−2728.
(2) Sansone, F.; Casnati, A. *Chem. Soc. Rev.* **2013**, *42*, 4623−4639.
(3) Dondoni, A.; Marra, A. *Chem. Rev.* **2010**, *110*, 4949−4977.
(4) André, S.; Sansone, F.; Kaltner, H.; Casnati, A.; Kopitz, J.; Gabius, H.-J.; Ungaro, R. *ChemBioChem* **2008**, *9*, 1649−1661.
(5) André, S.; Grandjean, C.; Gautier, F.-M.; Bernardi, S.; Sansone, F.; Gabius, H.-J.; Ungaro, R. *Chem. Commun.* **2011**, *47*, 6126−6128.
(6) Sansone, F.; Chierici, E.; Casnati, A.; Ungaro, R. *Org. Biomol. Chem.* **2003**, *1*, 1802−1809.
(7) Torvinen, M.; Neitola, R.; Sansone, F.; Baldini, L.; Ungaro, R.; Casnati, A.; Vainiotalo, P.; Kalenius, E. *Org. Biomol. Chem.* **2010**, *8*, 906−915.
(8) Sansone, F.; Baldini, L.; Casnati, A.; Ungaro, R. *Supramol. Chem.* **2008**, *20*, 161−168.
(9) Consoli, G. M. L.; Cunsolo, F.; Geraci, C.; Mecca, T.; Neri, P. *Tetrahedron Lett.* **2003**, *44*, 7467−7470.
(10) Consoli, G. M. L.; Cunsolo, F.; Geraci, C.; Sgarlata, V. *Org. Lett.* **2004**, *6*, 4163−4166.
(11) Avvakumova, S.; Fezzardi, P.; Pandolfi, L.; Colombo, M.; Sansone, F.; Casnati, A.; Prosperi, D. *Chem. Commun.* **2014**, *50*, 11029−11032.
(12) Becke, A. D. *J. Chem. Phys.* **1993**, *98*, 5648−5652.
(13) Lee, C.; Yang, W.; Parr, R. G. *Phys. Rev. B: Condens. Matter Mater. Phys.* **1988**, *37*, 785−789.
(14) Bryantsev, V. S.; Hay, B. P. *J. Phys. Chem. A* **2006**, *110*, 4678−4688.
(15) Cancés, E.; Mennucci, B.; Tomasi, J. *J. Chem. Phys.* **1997**, *107*, 3032−3042.
(16) Cossi, M.; Barone, V.; Cammi, R.; Tomasi. *Chem. Phys. Lett.* **1996**, *255*, 327−335.
(17) Barone, V.; Cossi, M.; Tomasi, J. *J. Comput. Chem.* **1998**, *19*, 404−417.
(18) Stoddart, J. F. *Calixarenes: An Introduction*; Gutsche, C. D., Ed.; The Royal Society of Chemistry: Cambridge, U.K., 2008; p 276.
(19) Arduini, A.; Fabbi, M.; Mantovani, M.; Mirone, L.; Pochini, A.; Secchi, A.; Ungaro, R. *J. Org. Chem.* **1995**, *60*, 1454−1457.
(20) As the molecular size of these mannosylthioureidocalix[4]arenes is too large to allow the location of the transition state corresponding to the arrow rotation at the chosen computational level, including the continuum solvent model, the energy barriers for the conversion of **1E**-*ZE* to its graph neighbor **1B**-*ZE*, as well as that between **2A**-*EZ* and **2B**-*EZ*, were estimated through a relaxed potential energy surface scan of the proper dihedral angle τ_1. The former barrier was shown to be 13−14 kcal/mol, whereas the latter was only ∼5 kcal/mol, thus indicating that the arrow rotation is much easier in **2** than in **1**.
(21) To estimate the energy barrier relative to the breathing equilibrium, a simplified structure, obtained from **2A**-*EZ* by deleting the four saccharide moieties, was optimized. It is expected that this simplification does not significantly alter the barrier value, as the sugars point outward with respect to the calix core. The corresponding transition state was also built and optimized both in vacuo and in water. Calculations showed an energy barrier of 7.81 kcal/mol that becomes even lower (6.14 kcal/mol) with solvation, thus highlighting the easiness of this interconversion.
(22) Frisch, M. J.; Trucks, G. W.; Schlegel, H. B.; Scuseria, G. E.; Robb, M. A.; Cheeseman, J. R.; Scalmani, G.; Barone, V.; Mennucci, B.; Petersson, G. A.; Nakatsuji, H.; Caricato, M.; Li, X.; Hratchian, H. P.; Izmaylov, A. F.; Bloino, J.; Zheng, G.; Sonnenberg, J. L.; Hada, M.; Ehara, M.; Toyota, K.; Fukuda, R.; Hasegawa, J.; Ishida, M.; Nakajima, T.; Honda, Y.; Kitao, O.; Nakai, H.; Vreven, T.; Montgomery, J. A., Jr.; Peralta, J. E.; Ogliaro, F.; Bearpark, M.; Heyd, J. J.; Brothers, E.; Kudin, K. N.; Staroverov, V. N.; Keith, T.; Kobayashi, R.; Normand, J.; Raghavachari, K.; Rendell, A.; Burant, J. C.; Iyengar, S. S.; Tomasi, J.; Cossi, M.; Rega, N.; Millam, J. M.; Klene, M.; Knox, J. E.; Cross, J. B.; Bakken, V.; Adamo, C.; Jaramillo, J.; Gomperts, R.; Stratmann, R. E.; Yazyev, O.; Austin, A. J.; Cammi, R.; Pomelli, C.; Ochterski, J. W.; Martin, R. L.; Morokuma, K.; Zakrzewski, V. G.; Voth, G. A.; Salvador, P.; Dannenberg, J. J.; Dapprich, S.; Daniels, A. D.; Farkas, O.; Foresman, J. B.; Ortiz, J. V.; Cioslowski, J.; Fox, D. J. *Gaussian 09*, revision B.01; Gaussian, Inc.: Wallingford, CT, 2010.

DOI: 10.1021/acs.joc.5b00878
J. Org. Chem. 2015, 80, 7412−7418